Global Change Biology
celebrating 20 years
Global Change Biology (2014), doi: 10.1111/gcb.12500

Cumulative geoecological effects of 62 years of infrastructure and climate change in ice-rich permafrost landscapes, Prudhoe Bay Oilfield, Alaska

MARTHA K. RAYNOLDS[1], DONALD A. WALKER[1], KENNETH J. AMBROSIUS[2], JERRY BROWN[3], KAYE R. EVERETT[4]†, MIKHAIL KANEVSKIY[5], GARY P. KOFINAS[6], VLADIMIR E. ROMANOVSKY[7,8], YURI SHUR[5] and PATRICK J. WEBBER[9]

[1]*Institute of Arctic Biology, University of Alaska Fairbanks, Fairbanks, AK 99775, USA,* [2]*Aerometric Geospatial Solutions, Anchorage, AK 99501, USA,* [3]*P.O. Box 7, Woods Hole, MA 02543, USA,* [4]*Byrd Polar Research Center, Ohio State University, Columbus, OH 43210, USA,* [5]*Department of Civil & Environmental Engineering, University of Alaska Fairbanks, Fairbanks, AK 99775, USA,* [6]*School of Natural Resources and Agricultural Sciences, University of Alaska Fairbanks, Fairbanks, AK 99775, USA,* [7]*Geophysical Institute, University of Alaska Fairbanks, Fairbanks, AK 99775, USA,* [8]*Earth Cryosphere Institute SB RAS, Box 1230, Tyumen, 625000, Russia,* [9]*P.O. Box 1230, Ranchos de Taos, NM 87557, USA*

Abstract

Many areas of the Arctic are simultaneously affected by rapid climate change and rapid industrial development. These areas are likely to increase in number and size as sea ice melts and abundant Arctic natural resources become more accessible. Documenting the changes that have already occurred is essential to inform management approaches to minimize the impacts of future activities. Here, we determine the cumulative geoecological effects of 62 years (1949–2011) of infrastructure- and climate-related changes in the Prudhoe Bay Oilfield, the oldest and most extensive industrial complex in the Arctic, and an area with extensive ice-rich permafrost that is extraordinarily sensitive to climate change. We demonstrate that thermokarst has recently affected broad areas of the entire region, and that a sudden increase in the area affected began shortly after 1990 corresponding to a rapid rise in regional summer air temperatures and related permafrost temperatures. We also present a conceptual model that describes how infrastructure-related factors, including road dust and roadside flooding are contributing to more extensive thermokarst in areas adjacent to roads and gravel pads. We mapped the historical infrastructure changes for the Alaska North Slope oilfields for 10 dates from the initial oil discovery in 1968–2011. By 2010, over 34% of the intensively mapped area was affected by oil development. In addition, between 1990 and 2001, coincident with strong atmospheric warming during the 1990s, 19% of the remaining natural landscapes (excluding areas covered by infrastructure, lakes and river floodplains) exhibited expansion of thermokarst features resulting in more abundant small ponds, greater microrelief, more active lakeshore erosion and increased landscape and habitat heterogeneity. This transition to a new geoecological regime will have impacts to wildlife habitat, local residents and industry.

Keywords: Arctic, climate change, cumulative impacts, geoecological mapping, ice-rich permafrost, ice-wedge polygons, infrastructure, photo-interpretation, thermokarst, tundra

Received 18 September 2013 and accepted 8 November 2013

Introduction

Oil and gas exploration and extraction are occurring in ice-rich permafrost (IRP) areas of Alaska, Canada, and Russia, and it is inevitable that more extensive networks of infrastructure than presently exist will be required to extract the resources of these areas (AMAP, 2010). These will be constructed against a backdrop of rapid climate change, rapid technological changes, and unpredictable social-ecological changes (Truett & Johnson, 2000; Orians *et al.*, 2003; ACIA, 2005; AMAP, 2010; Krupnik *et al.*, 2011; Kofinas *et al.*, 2013). Documenting the history of these developments as they occur will aid local communities, researchers, land managers, industry, and policy makers in developing adaptive approaches to plan for and respond to future changes (AMAP, 2010; Streever *et al.*, 2011).

Correspondence: Martha K. Raynolds, 311 Irving, Institute of Arctic Biology, University of Alaska Fairbanks, Fairbanks, AK 99775, USA, tel. + 907 474 6720, fax + 907 474 7666, e-mail: mkraynolds@alaska.edu
†Deceased.

The Prudhoe Bay Oilfield

The Prudhoe Bay Oilfield (PBO) in northern Alaska was the first developed oilfield in the Arctic, and is the largest in the United States. It is an extremely important

asset to the United States and the state of Alaska, containing 16% of US proven reserves of oil and gas (Alaska Oil & Gas Association, 2012; USEIA, 2012). In 2012, taxes on the oil from the Northern Alaska oilfields accounted for over 90% of the Alaska state budget (Alaska Oil & Gas Association, 2012). The PBO is located on the Beaufort Sea coast, halfway between the Canadian border and Point Barrow, a region that was remote and roadless prior to the discovery of oil in March 1968. An extensive infrastructure network quickly grew following the oil discovery, resulting in development within an approximately 2600 km^2 area (Fig. 1a).

Oilfield engineering evolved rapidly in response to the IRP conditions encountered (Gilders & Cronin, 2000; Orians *et al.*, 2003). Gravel construction pads over 2-m thick were used to insulate the frozen tundra. Since 1995, new technologies, including much closer spacing of the well heads, directional drilling to reach deposits up to 6.4 km from the drilling sites, and reinjection of drilling fluids into the geological formations to eliminate the need for reserve pits, considerably reduced the size of gravel pads for drill sites in newer oilfields. The use of winter ice-roads and roadless access to drill sites have further reduced the footprint of modern oilfields (Gilders & Cronin, 2000; AMAP, 2010; Streever *et al.*, 2011).

The early phase of PBO development stimulated geoecological and permafrost research in the region by the Tundra Biome investigations of the International

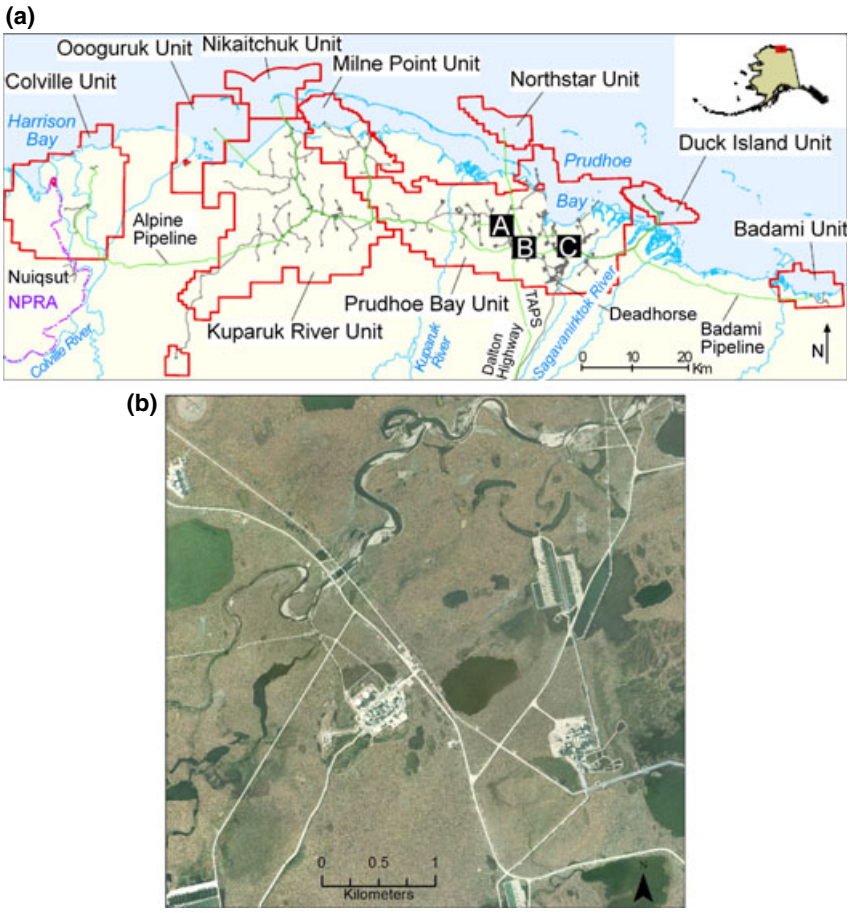

Fig. 1 Alaska North Slope production units that comprise the Prudhoe Bay Oilfield referred to in this article. (a) Major oil production units (red boundaries) and extent of infrastructure. Gray lines are gravel roads, airstrips, and construction pads. Green lines are major pipelines. Small black squares A, B, and C are locations of the detailed 20-km^2 map areas of this study. Note the Iñupiat village of Nuiqsut at left in the National Petroleum Reserve Alaska, the Trans-Alaska Pipeline System and Dalton Highway that link the oilfields to southern Alaska. *Inset*: Location within Alaska. Map courtesy of Aerometric, Inc. and BP Alaska, Inc. (b) Map B, showing the meandering Putuligayuk River and its floodplain, thaw lakes, drained lake basins, and primary surfaces between lakes. The infrastructure consists of a network of roads, drill sites, and processing facilities. The width of the area shown is 4.7 km. See Fig. 5 for geoecological and historical change maps of this area. Imagery courtesy BP Exploration (Alaska), Inc.

Biological Programme (Brown, 1975, 1980; Walker *et al*., 1980); and the Circumpolar Active-Layer Monitoring Program (Brown *et al*., 2000). Although the oil industry states that the density and extent of the infrastructure of the PBO will likely not be replicated in new oilfields, we focused our studies here because it has the longest history of development and scientific research, and is the only area with detailed time-series of geoecological and historical-change maps that span the complete history of the field. Many of the types of landscape change seen here, such as those associated with roads and climate change, will occur in other IRP areas.

IRP terrain and thermokarst

The PBO region is a showcase of periglacial landforms, including thaw lakes, pingos, meandering beaded streams, and many types of patterned ground such as nonsorted circles, and ice-wedge polygons indicative of IRP (Everett, 1980a). Within this landscape, ground-ice formation and thawing occurs in a hierarchy of time and space scales ranging from daily needle-ice formation to annual processes associated with frost-heave features (e.g., frost boils) to centuries and millennia involved with ice-wedge-polygon and thaw-lake formation (Walker, 2000). These processes create a mosaic of exceptionally dynamic landforms, soils, and vegetation that are susceptible to abrupt changes, especially if the features are disturbed by mechanical means or by rapid climate change (Lawson *et al*., 1978; Lawson, 1982; Komárková & McKendrick, 1988; Walker, 1996, 1997; Callaghan *et al*., 2005; Shur & Jorgenson, 2007; Shur & Osterkamp, 2007; Grosse *et al*., 2011).

Permafrost is ground (soil or rock, in most cases including ice) in which a temperature below 0 °C exists for two or more years (Van Everdingen, 1998). At Prudhoe Bay, permafrost is continuous and extends to a depth of 660 m (Gold & Lachenbruch, 1973). The *active layer*, the layer of soil near the surface that thaws annually, varies in thickness from about 0.25 m in peaty soils near the coast to over 2 m on some south-facing gravelly slopes and averages about 0.5 m (Everett, 1980b). IRP has a high percentage of *excess ice*, where the ice in the ground exceeds the total pore volume that the ground would have under unfrozen conditions (Van Everdingen, 1998). Although IRP has high load-bearing capacity if its thermal stability is maintained, it has none if the excess ice melts. Nearly all of the developed and developing oil and gas fields in arctic Alaska, Canada, and Russia are in regions with extensive IRP.

Much of the excess ice in the Prudhoe Bay permafrost is in the form of ice-wedges, which occupy on average 11% of the total volume of the upper 2–3 m of permafrost for all sites studied along the Beaufort coast, but which can reach 30% in some areas of the Arctic Coastal Plain of Alaska (Everett, 1980b; Kanevskiy *et al*., 2013). The average total volumetric ice content, including the wedge ice, segregated ice, and pore ice, exceeds 80% on all terrain units studied except in sand dunes and deltas (Kanevskiy *et al*., 2013).

If the insulative vegetated mat over ice wedges is disturbed or if other causes introduce heat to the ice-wedges (e.g., standing or flowing water), thawing of the ice will result in settling of the surface and creation of *thermokarst terrain* (Fig. 2) (Van Everdingen, 1998). Although thermokarst is not a form of karst, the subsidence and collapse associated with thermokarst terrain has some analogies to karst topography (French, 1976). Considerable research has been devoted to defining the hazards of thermokarst to structures (Nelson *et al*., 2002) and in the development of engineering solutions to avoid thermokarst formation (US Arctic Research Commission Permafrost Task Force, 2003).

Within the PBO, most of the extremely IRP occurs within approximately 2 m of the surface, in frozen, organic-rich silts that overlie more stable alluvial sands

Fig. 2 Flooding and thermokarst along roads at Prudhoe Bay, AK. (a) Typical roadside environment showing flooded troughs and resulting thermokarst terrain. Heavy road dust killed vegetation on the centers of ice-wedge polygons near the road. (b) Thermokarst with active erosion of resulting high-centered polygons and widening of polygon troughs, near a gravel road. (c) Aerial photograph of flooding of ice-wedge polygon troughs due to blocked drainage. Previous low-centered ice-wedge polygons were converted to high-centered polygons. *Photos*: D.A. Walker, 1 July 2013.

and gravels (Everett, 1980b; Rawlinson, 1993) (Fig. SA1). See Supporting Information, Appendix S1, for further explanation of IRP in the PBO with photographs of segregated ice and a cross–section of a 100-m trench illustrating the types and amount of ice in the substrate (Fig. SA5).

Scattered small *thermokarst pits* were mapped during the baseline geobotanical mapping in the PBO (Walker *et al*., 1980). These small near-circular ponds commonly overlie the intersections of ice wedges, most commonly on *primary surfaces* (old landscapes unaltered by thaw-lake or river processes) (Sellmann *et al*., 1975), wherever there has been time for large ice-wedges to form (Fig. SA6a). These pits have been identified in the Russian literature as the first step in thermokarst development (Shur & Osterkamp, 2007). Until recently, the thermokarst pits in natural landscapes at PBO appeared to be fairly stable because most of the pits noted in the 1970s were also visible on the 1949 aerial photographs and showed little change through 1990 (Fig. 3). Recent abrupt changes in thermokarst pit size and density were documented in the Fish Creek region, about 40 km west of the PBO. These changes were thought to be a response to a period of warm summer temperatures during the 1990s (Jorgenson *et al*., 2006). As discussed below, our study documents a similar trend in thermokarst in the PBO.

Cumulative effects of oil development

The effects of oil and gas activities take different forms in different parts of the Arctic, where environmental and social conditions vary. Summaries of some of the cumulative effects have been addressed in Russia (Forbes *et al*., 2009; Walker *et al*., 2011; Kumpula *et al*., 2012), Alaska (Walker *et al*., 1987; Orians *et al*., 2003), and globally (AMAP, 2010). The cumulative effects of oil development were first studied at Prudhoe Bay in the 1980s with mapping that quantified the extent of direct and indirect landscape effects of oilfield infrastructure (Walker *et al*., 1986a,b, 1987). *Direct effects* were defined as physical changes that were planned in advance, such as roads, gravel pads, and gravel mines. The unplanned *indirect effects* were more difficult to anticipate (Walker *et al*., 1987; Shur, 1988). They often occurred in areas adjacent to infrastructure and

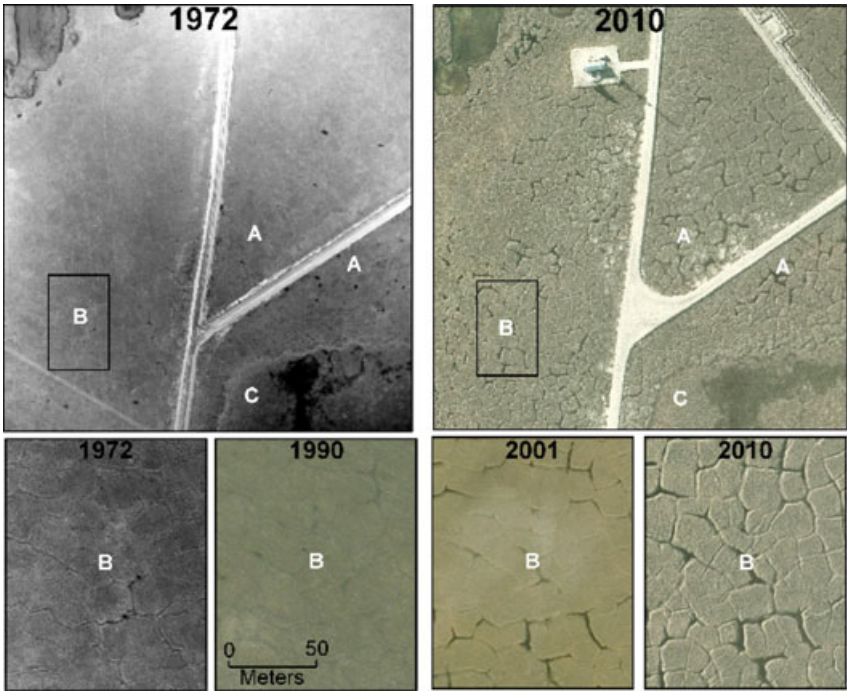

Fig. 3 Changes between 1972 and 2010 near the main road junction in map B. Note changes in infrastructure, including small new gravel pad and building near the top of the photo, a new pipeline and gravel road on the upper right side, and an expanded road intersection. Also note extensive changes in the character of the ice-wedge polygons with many more flooded ice-wedge troughs between polygons in 2010. Areas near A and B have extensive ice-wedge polygons. Numerous scattered small thermokarst pits (small dark ponds) are visible near A in 1972, with little change in 1990. Areas A and B and show marked increases in thermokarst in 2001 and even more by 2010. Area C is in a drained thaw lake basin with ice-poor soils and shows little evidence of new thermokarst. Changes in area A were mapped as infrastructure-related because of the proximity of the road and the pipeline that have significantly altered the hydrology of this area. Area B is not clearly affected by infrastructure.

included roadside dust, infrastructure-related flooding, off-road vehicle traffic, and thawing of near-surface permafrost (Walker *et al*., 1987) (Appendix S3).

A 2003 US National Research Council (NRC) study of the cumulative effects of oil development on Alaska's North Slope (Orians *et al*., 2003) included a time-series inventory of the total extent of infrastructure on the North Slope (Ambrosius, 2003). Although the NRC study recognized that climate change would likely have numerous effects to sea ice and Arctic ecosystems, the report concluded that climate change would not seriously affect oil and gas activities on the North Slope (Orians *et al*., 2003). This was based largely on the assumption that cold, continuous permafrost, such as that found in the PBO, is robust and not likely to thaw even if the permafrost temperatures were raised several degrees. Since the NRC study, several regional studies have pointed to terrain and vegetation changes related to climate change (Sturm *et al*., 2001; Jia *et al*., 2003; Bhatt *et al*., 2010; Myers-Smith *et al*., 2011; Epstein *et al*., 2012; Tape *et al*., 2012), including recent thawing of the near-surface permafrost (Jorgenson *et al*., 2006).

Here, we update both the regional assessment of total infrastructure extent from the NRC report (Orians *et al*., 2003) and the analysis within three 20-km^2 areas previously analyzed in 1983 (Fig. 1) (Walker *et al*., 1987). This article addresses the questions 'How have oilfield infrastructure and climate change affected the IRP landscapes of the PBO over 62-year of observations?' And 'How have the initial geoecological conditions in the region affected the changes?'

Materials and methods

Total North Slope oilfield infrastructure footprint

BP Exploration (Alaska) Inc. maintains a time series of aerial photographs and a set of topographic base maps (map scale 1 : 6000) of the PBO. Aerial photos taken in 1968 were used to define the areas prior to most development. Infrastructure changes were added from each successive analysis year (1973, 1977, 1983, 1988, 1994, 2001, 2006–2007, 2010, and 2011), creating CAD files for calculating incremental changes for the area shown in Fig. 1a. The files contained the areas covered by gravel facilities, roads, and mine excavations. Indirect effects, exploration facilities, riverbed gravel extraction, and other impacted areas not covered by gravel facilities were not included on these maps. Calculations were performed using ARC View software in an Alaska State Plane, zone 4, NAD27 projection (Appendix S2).

Integrated geoecological and historical change maps

A detailed mapping approach was used to examine both direct and indirect landscape changes within three 20-km^2 areas (A, B, C, example shown in Fig. 1b). The set of aerial photo missions used for the analysis included the years 1949, 1968, 1970, 1972, 1973, 1977, 1979, 1983, 1990, 2001, and 2010 (Table SC1). The methods used in the first analysis of cumulative effects of oil development (Walker *et al*., 1986a,b) were modified for this update to take advantage of new advances such as heads-up digitizing, GIS database formatting and improved infrastructure maps of the region. The database contained polygons coded with nine geoecological attributes: dominant vegetation, secondary vegetation, tertiary vegetation; percentage open water; landform; dominant surface form, secondary surface form; dominant soil, and secondary soil (Table SC2). Secondary and tertiary variables were mapped if they covered more than 30% of a map polygon. Eighteen infrastructure-related change attributes, and six non-infrastructure-related change attributes were also mapped (Table SC2).

Results

North Slope oilfield infrastructure footprint

Results for the entire oilfield are presented by number of infrastructure items, length of linear infrastructure items, and area covered by facilities (Fig. 4a–c respectively). As of 2011, there were 127 production pads, 25 facility pads, 145 support pads (power stations, camps staging areas, etc.), 103 exploration sites, 13 offshore exploration islands, 7 offshore production islands, 9 airstrips, 4 exploration airstrips, 2037 culverts, 27 bridges, 50 caribou crossings, and one active landfill. The number of these infrastructure items increased rapidly between 1968 and 1983 and more slowly since then. The number of exploration pads decreased slightly after 2001, but increased again after 2007 (Fig. 4a and Table SB1).

The road network consisted of 669 km of gravel roads, 154 km of abandoned peat roads, 12 km of causeways, 96 km of abandoned tractor trails, and 54 km of exploration roads with thin gravel or tundra scars. Similar to the number of facilities, the total length of roads increased rapidly until 1988 and then leveled off at 931 km (Figs 1a and 4b). The 790-km pipeline network includes groups of parallel pipelines elevated 1–2 m above the tundra surface on vertical supports. Pipeline corridors included anywhere from 1 to 21 closely spaced parallel pipelines with diameters up to 60 cm. The length of major powerlines with towers totaled 541 km (Table SB1).

The total oilfield infrastructure covered 7429 ha of the North Slope by 2011, mainly consisting of 2345 ha of gravel pads, 2737 ha of gravel mines, and 1255 ha of gravel roads and causeways (Fig. 4c). Impacted areas also included airstrips (125 ha), offshore gravel pads and islands (82 ha), exploration sites (290 ha),

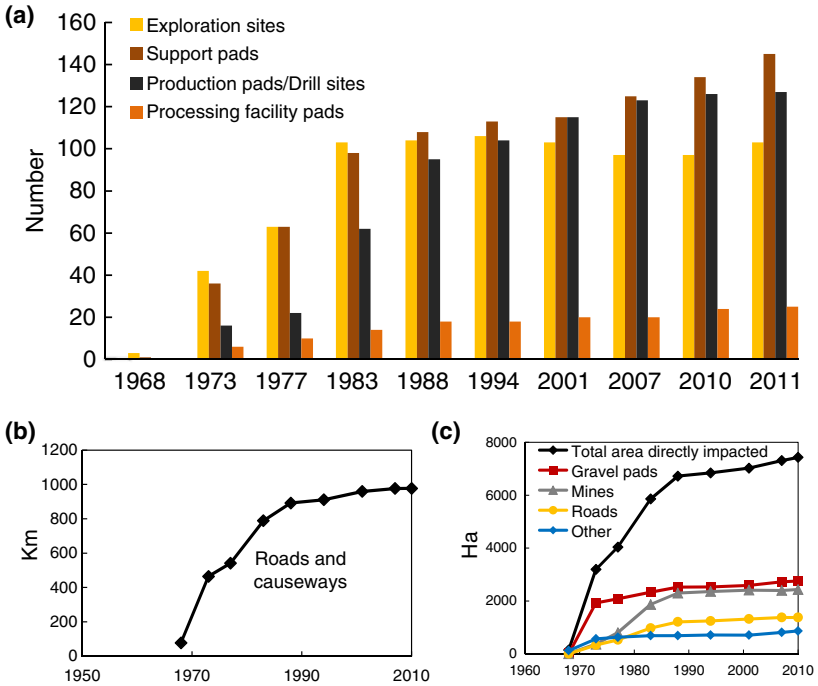

Fig. 4 History of infrastructure on the North Slope oilfields 1968–2011 (excluding the Dalton Highway and Trans-Alaska Pipeline System). (a) Number of infrastructure items, (b) total length of roads (km), (c) directly impacted area (ha). Data courtesy of Aerometric, Inc. and BP Exploration (Alaska), Inc.

exploration airstrips (20 ha), peat roads (209 ha), tractor trails/scars (104 ha), exploration roads (72 ha), and areas where pads have been removed and are in the process of recovery (190 ha). Most of the direct effects to the landscape occurred within 18 years of the initial discovery of oil, reaching 6722 ha by 1988 (Fig. 4c). Since 2001, the oil development has expanded westward, increasing the infrastructure area to 7429 ha (Table SB1).

Direct and indirect effects of infrastructure in maps A, B, and C

Thematic maps for area B show the dominant vegetation, landforms, and surface forms prior to development (Fig. 5). The landform map is overlaid with the major infrastructure-related changes (Fig. 5c). Area B is of special interest because it was the focus of the International Biological Programme Tundra Biome studies and several other scientific studies at Prudhoe Bay (Brown, 1975; Everett & Parkinson, 1977; McKendrick, 1987, 1991; Walker *et al.*, 1987; Walker & Everett, 1991) and contains Pump Station 1, the start of the Trans-Alaska Pipeline System. Thematic maps for all three map areas (A, B, and C) portray surface forms, landforms, dominant vegetation, soils, percent water, total infrastructure-related effects, and total noninfrastructure-related effects (Fig. SC4–SC6).

Time series of maps portraying infrastructure-related changes (Fig. SC7–SC9) showed that the progression of area impacted by direct effects on maps A, B, and C (Fig. 6a) was similar to that in the larger North Slope area (Fig. 4), except that this area was the first to be developed and construction leveled off within 15 years (by 1983 instead of by 1988 as was the case for the regional infrastructure) and declined some afterwards as a few sections of roads were removed and revegetated and some areas of gravel mining in rivers were no longer detectable. The total area of direct effects in 2010 on the three detailed maps was 919 ha (14.6%), ranging from 12.2% in map A to 19.3% in map C (Table SC5). Gravel pads covered the most area (438 ha), followed by excavations (257 ha), roads (136 ha), and pipelines (79 ha) (Fig. 6a and Table SC5).

The total area of indirect effects of oilfield development exceeded the direct effects by 1977, and showed an almost linear rate of increase of about 23 ha year^{-1} in the most recent twenty years (1990–2010), resulting in a total of 1794 ha (28.6% of the area of the three maps), about double the area of the direct effects (919 ha) (Fig. 6a and Table SC5). By 2010, indirect effects included 701 ha of flooding, 367 ha of infrastructure-related thermokarst, 332 ha of gravel and

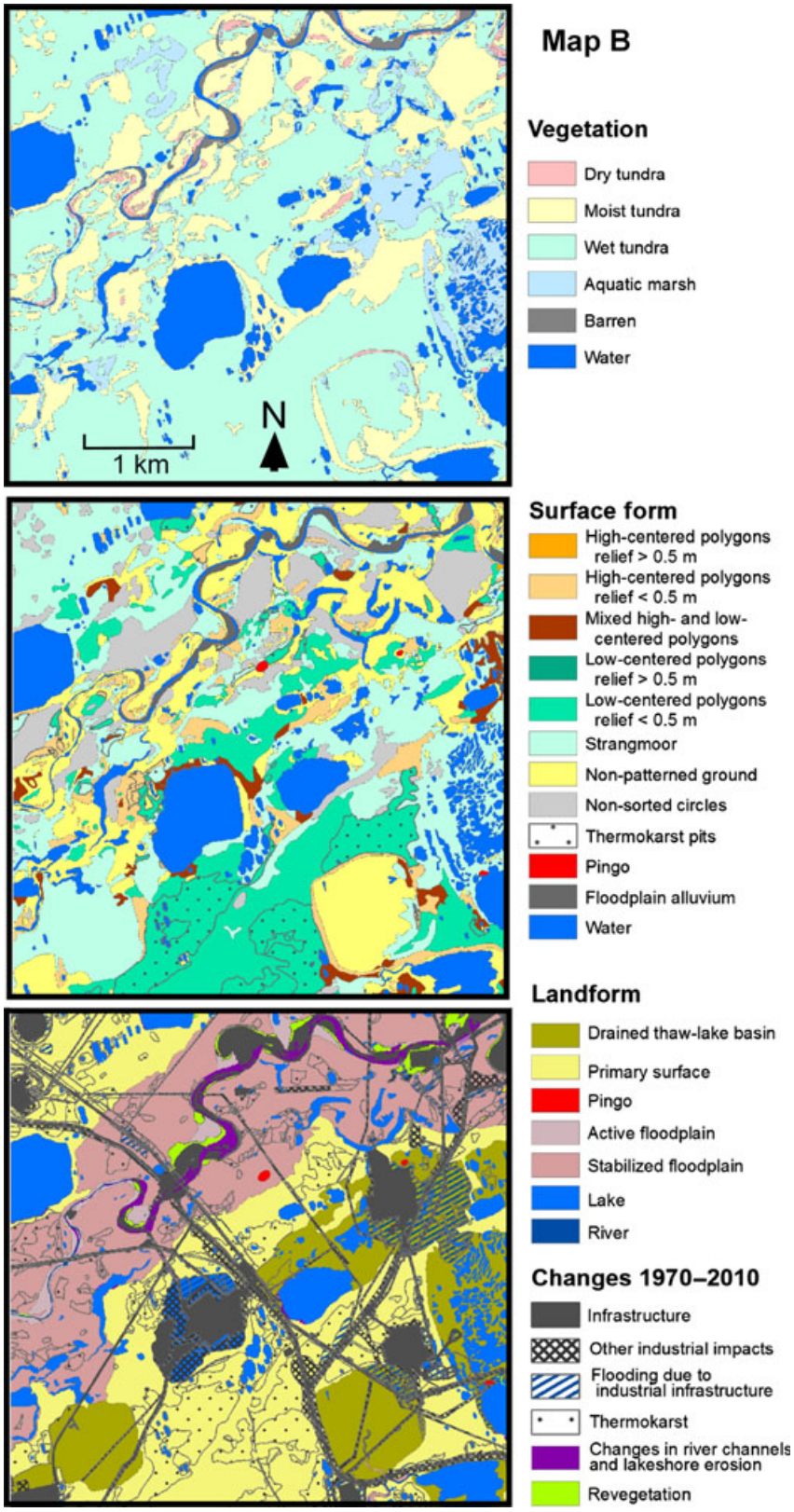

Fig. 5 Dominant vegetation types, surface forms, and landforms with mapped changes (1968–2010) for 20-km^2 area of the Prudhoe Bay oilfield (map B on Fig. 1). See Fig. SC4–S-C6 for full sets of thematic maps for maps A, B, and C.

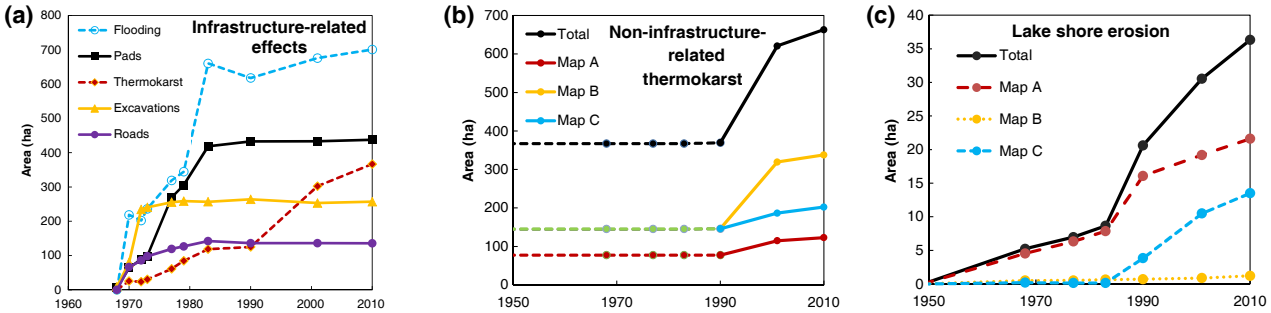

Fig. 6 History of changes (1949–2010) in three 20-km^2 mapped areas within Prudhoe Bay Oilfield, North Slope, Alaska: (a) history of most common infrastructure-related effects – direct effects (solid lines) and indirect effects (dashed lines); (b) history of noninfrastructure-related thermokarst and (c) history of lake-shore erosion for maps A, B, and C and for the total mapped area (60 km^2). See Fig. SC7–S-C9 for maps of these changes.

debris adjacent to roads and pads, 291 ha of off-road vehicle tracks, and 34 ha of road dust (Table SC5). The extent of road dust and vehicle trails is underrepresented in the data because they were difficult to detect at the scale of mapping. Furthermore, these factors were most often mapped as secondary or tertiary effects in areas where flooding and thermokarst occurred and thus do not show up as the dominant factors, which are summarized here.

Flooding developed quickly as roads and pipelines spread across the flat PBO landscape and dammed the flow of runoff waters during the spring melt season. The extent of flooding nearly leveled off after 1983 at over 650 ha of maps A, B, and C (Fig. 6a). By 2010, the area of infrastructure-related flooding ranged from 25.1% of map A (an extremely flat area with many thaw lakes) to 2.0% of map C (a relatively well-drained area close to the Sagavanirktok River).

Thermokarst, the second most extensive indirect effect, began developing in roadside areas soon after the roads were built (Fig. 2). Visible on the aerial photographs as increased standing water in polygon troughs and subsidence of polygon edges, thermokarst initially covered rather small areas, but expanded at a linear rate over the entire history of the field (9.2 ha year^{-1}, $r^2 = 0.96$). After 42 years, within maps A, B, and C, 367 ha of tundra near infrastructure had thermokarst (Fig. 6a). Road dust in high concentrations adjacent to the more heavily traveled roads kills much of the vegetation (Fig. 2a), especially the low-growing mosses and lichens, decreasing the insulative value of the vegetation, and greatly increasing the active-layer thickness (ALTs) and susceptibility of the tundra to thermokarst (Walker & Everett, 1987). In winter, snow drifts develop along both sides of the elevated road berms, resulting in warmer winter soil temperatures near the roads, which increases ALTs and thermokarst in areas adjacent to infrastructure. Road dust in the snow reduces its albedo and leads to early snow melt next to the roads (Benson *et al.*, 1975), increased roadside flooding, and deeper ALTs (Walker & Everett, 1987).

Changes not related to infrastructure

Numerous changes that cannot be attributed to oilfield development also occurred (Fig. 6b, c), including thermokarst far from facilities, erosion of lake shorelines, and erosion, deposition, and revegetation of river bars and banks along the Putuligayuk and Sagavanirktok Rivers. The total area affected by these changes by 2010 was 687 ha (11% of the three mapped areas, Table SC5). While erosional and depositional changes in the rivers mostly compensated for each other, trends for thermokarst (Fig. 6b) and lakeshore erosion (Fig. 6c) were unidirectional.

Lakeshore erosion totaled 36 ha, 0.6% of the mapped area by 2010 (Fig. 6c). Lakeshore erosion showed an abrupt increase in recent years, as was seen with noninfrastructure-related thermokarst. There was a slow, steady increase in lakeshore erosion between 1949 and 1983, reaching 8.6 ha on maps A, B, and C; then to 36 ha from 1983 to 2010, more than a fourfold increase in 27 years (Fig 6c).

The most extensive noninfrastructure-related change was thermokarst, visible as increased standing water in the troughs of ice-wedge polygons (Figs 2 and 3), which covered 503 ha by 2010, 8% of the three mapped areas (Table SC5 and Fig. SC7h–S-C9h). Thermokarst in areas distant from infrastructure increased from 367 ha in 1968 to 663 ha in 2010 (Fig. 6b). The area of thermokarst did not noticeably increase between the late 1960s and 1990 on any of the maps (e.g. Fig. 3), but increased 1.8-fold between 1990 and 2010.

By 2010, noninfrastructure-related thermokarst occurred on 19.1% of the areas unaffected by development where thermokarst potentially could occur (i.e.,

excluding lakes and active floodplains). The landforms most affected by noninfrastructure-related thermokarst were primary surfaces between thaw lakes (residual surfaces not affected by thaw-lake processes), and stabilized river floodplains (31.3% and 16.2%, respectively, Fig. 7, Table SC6). Drained thaw lakes showed little increase in thermokarst features. Surface forms showed a wide range of responses. Low-centered polygons with <0.5 m elevation contrast between the center and the rim, and areas with mixed high- and low-centered polygons were most affected by thermokarst (46.1% and 45.7%, respectively), whereas only 26.0% of high-centered polygons with <0.5 m center-trough contrast had enhanced thermokarst (Fig. 7). Of the area without industrial effects and mapped as having thermokarst pits in 1968, 54% showed increased thermokarst by 2010. Wet tundra and moist tundra were the vegetation types showing the most nonindustrial thermokarst (23.9% and 16.7%, respectively); no other vegetation type had over 5% affected by increased thermokarst. Wet, patterned-ground soil associations showed the most increase in thermokarst (37.6%, Fig. 7 and Table SC6). The total area where increased thermokarst was detected, including infrastructure-related and noninfrastructure-related thermokarst was 870 ha (13.9% of the mapped area).

Discussion

Relationship of thermokarst to air and soil temperatures, ALT, and precipitation

The documented regional increase in thermokarst is most likely due to a long-term upward trend in summer temperatures and to the exceptionally warm summers of 1989 and 1998 (Fig. 8). Summer air temperatures as indicated by the summer warmth index (SWI = sum of monthly mean air temperatures above 0 °C, or thawing degree months [°C mo]) increased about 5 °C mo over the 1970–2012 period of record at the Deadhorse airport (Fig. 8). Similar trends are seen in the long-term records from Barrow and Umiat (Jia *et al.*, 2003). The highest recorded SWI at Deadhorse occurred in 1989 and 2012 (30.7 °C mo, 30.5 °C mo), and the third highest was in 1998 (27.5 °C mo). The average SWI for the period 1970 to 1999 was 19 °C mo. The 1989 and 1998 SWI peaks at Deadhorse are similar to the magnitude of thawing-degree-day peaks at the Kuparuk Airport, 100 km west of the study area (Jorgenson *et al.*, 2006).

The mean annual air temperature (MAAT), mean annual permafrost temperature at the upper surface of the permafrost ($MAPT_S$), and at 20-m depth ($MAPT_{20}$),

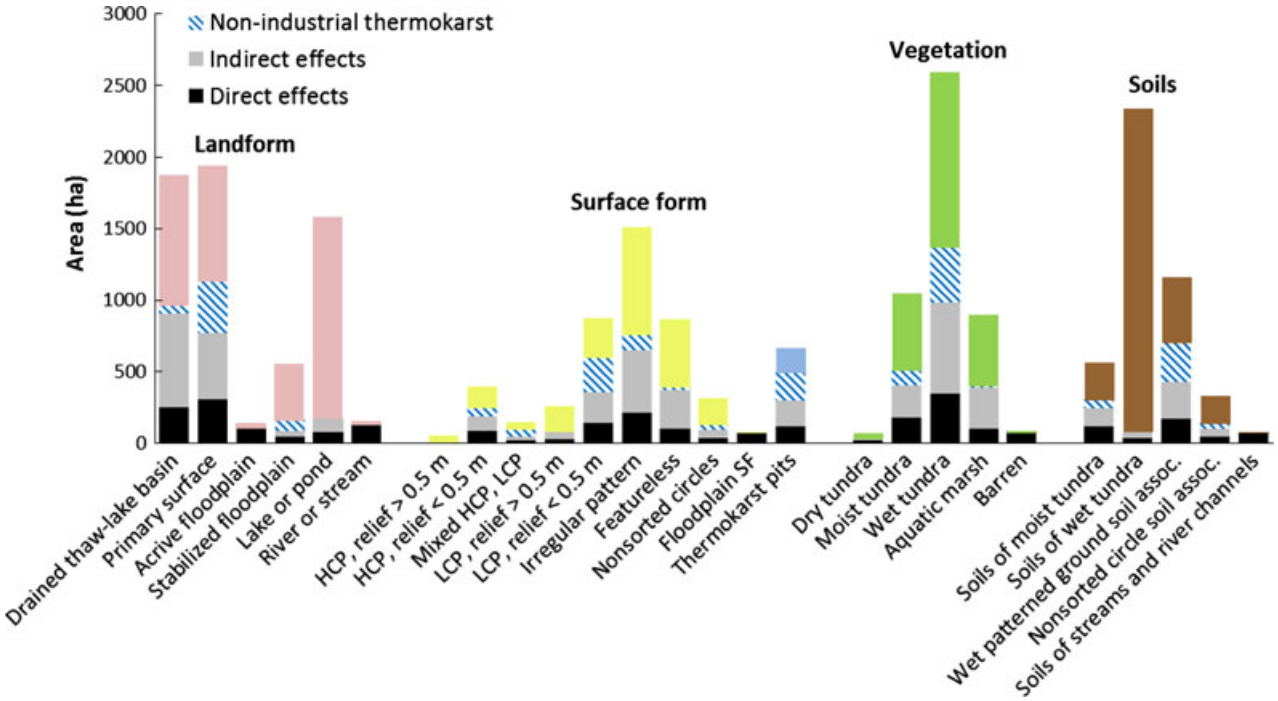

Fig. 7 Total areas of geoecological units >50 ha within maps A, B, and C, area of each unit with direct (black) and indirect (gray) industrial impacts, with nonindustrial thermokarst (blue diagonal stripes) and remaining unchanged portion (includes area of floodplain gravel erosion and deposition). Thermokarst pits include areas mapped with this code as dominant or secondary surface form. HCP, high-centered polygons; LCP, low-centered polygons; SF, surface form. See Supporting Information Table C6 for tabular summary.

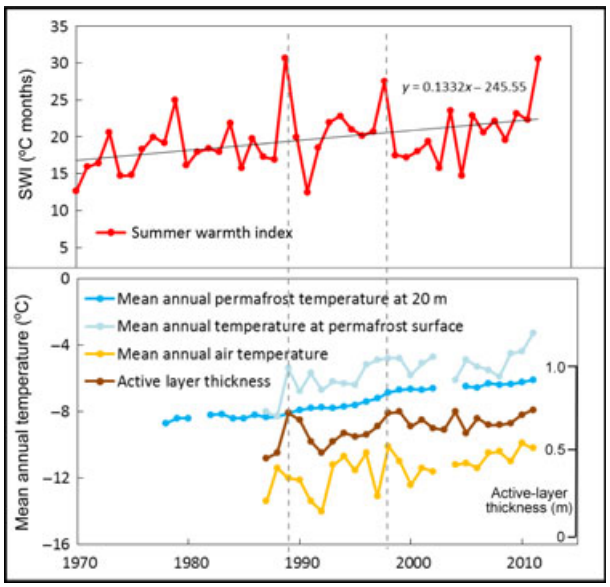

Fig. 8 *Top*: Trend of summer air temperature as indicated by the summer warmth index (SWI = Sum of the monthly mean temperatures above freezing, °C mo). Data are from the Western Regional Climate Center, Prudhoe (1970–1986) and Deadhorse (1987–2012). *Bottom:* Mean annual air temperature at 2 m height (MAAT, orange line), mean annual permafrost temperature at 20-m depth ($MAPT_{20}$, dark blue line), mean annual temperature at the upper surface of permafrost ($MAPT_s$, light blue line); and active layer thickness (ALT, brown line and scale on right). All data are from Osterkamp and Romanovsky Deadhorse station. The climate station and maps (A, B, and C) are within 15 km of each other. Active layer depth was measured by interpolation of soil temperature data from several depths for 1987–1996 and by using a metal probe for 1997–2011. Note the corresponding peaks in SWI, ALT, and $MAPT_s$ in the extreme warm summers of 1989 and 1998 (gray dashed lines). Trend lines are as follows: SWI = 0.1332 year − 245.55; $MAPT_{20}$ = 0.082 year − 170.9; $MAPT_s$ = 0.1089 year − 223.37; MAAT = 0.0918 year − 194.92; ALT = 0.0665 year − 141.85.

and ALT all increased markedly (Fig. 8). The period of most rapid increase in all these variables was during the 1990s. The rate of increase declined from 2001 to 2010, corresponding to a period of moderate air temperatures. Records of ALT from CALM grids at West Dock and Deadhorse also showed maximum thaw depths in 1998, followed by less deep summer thaws in the following decade (Shiklomanov *et al*., 2012).

Increases in ALT can trigger thawing of ground ice in the upper permafrost, including the top parts of the ice wedges, which can result in the formation of water-filled thermokarst troughs above ice wedges. However, the expansion of thermokarst pits into a network of flooded ice-wedge-polygon troughs as documented in this study may also be related to thermal feedbacks associated with flooding of the troughs. We find no indication that the increase in surface water visible in the ice-wedge polygon troughs in the recent aerial photographs from 1990, 2001, and 2010 was due to higher water tables or to exceptionally wet years. No change in lake levels was detected on the aerial photographs. Furthermore, precipitation records over the 1991–2000 and 2001–2010 period averaged 10.6 and 9.9 cm $year^{-1}$, respectively, with values for the years of the aerial photography at 7.4 cm in 1990, 7.4 cm in 2001, and 3.9 cm in 2010 (WRCC, 2012). Modeled Prudhoe Bay Region ALTs for 1992–2000 showed an exceptionally deep active layer in 1998, and a trend of subsidence of the ground surface caused by the melting of soil ice (Liu *et al*., 2012). The similarity of thermokarst patterns in the PBO with those detected west of the oilfield (Jorgenson *et al*., 2006) indicates that regional climate change is the most likely cause of thermokarst.

Relationship of thermokarst to mapped geoecological features

The occurrence of thermokarst is not uniformly distributed across the landscape and was to some extent predictable based on the earlier geoecological mapping. Areas mapped on the 1968 imagery as 'primary surfaces', 'low-centered ice-wedge polygons', 'wet sedge, moss tundra', 'wet patterned-ground soil association', and 'thermokarst pits' were the most susceptible to further thermokarst. Most of the thermokarst is occurring on surfaces that have not experienced recent lake drainage or reworking of riparian sediments, and are old enough to have accumulated large volumes of excess ice in the form of ice wedges and segregated ice. High-centered ice-wedge polygons experienced less change than low-centered polygons, most likely because these areas have experienced previous thawing and subsidence of ice wedges. Accumulation of organic and mineral matter in the troughs probably helped to protect these ice-wedges from additional thawing (Jorgenson *et al*., 2006), making these areas less susceptible to the present-day climate change.

A planning process for siting new infrastructure that recognizes the susceptibility of different landforms, vegetation types, and soils to flooding and thermokarst would help to minimize these effects.

A conceptual model of infrastructure-related and climate-change-related thermokarst

Thermokarst development is a complex process that includes numerous positive and negative feedbacks. Thermokarst in areas of IRP with near-surface ice wedges can follow two distinctly different scenarios (Fig. 9). Both scenarios start with partial thawing of the

upper ice wedges and formation of small shallow ponds (thermokarst pits) in the troughs over ice wedges and especially at ice-wedge intersections. This initial stage of thermokarst development is triggered by an increase in the ALTs caused by higher than normal air temperatures, flooding, or destruction of vegetation.

The first (stable or reversible) scenario (Fig. 9, blue arrows) is often observed in a natural environment and is described in part by Jorgenson *et al.* (2006). This scenario is possible when the ice wedges are affected by thermokarst, while the polygon centers remain relatively stable because of an undisturbed insulative mat of vegetation and soils. An increase in the ALTs in the polygon centers usually results only in moderate surface subsidence due to partial thawing. Over time, mineral and organic matter accumulate in the troughs from erosion of the trough margins and increased plant productivity due to a combination of deeper thaw,

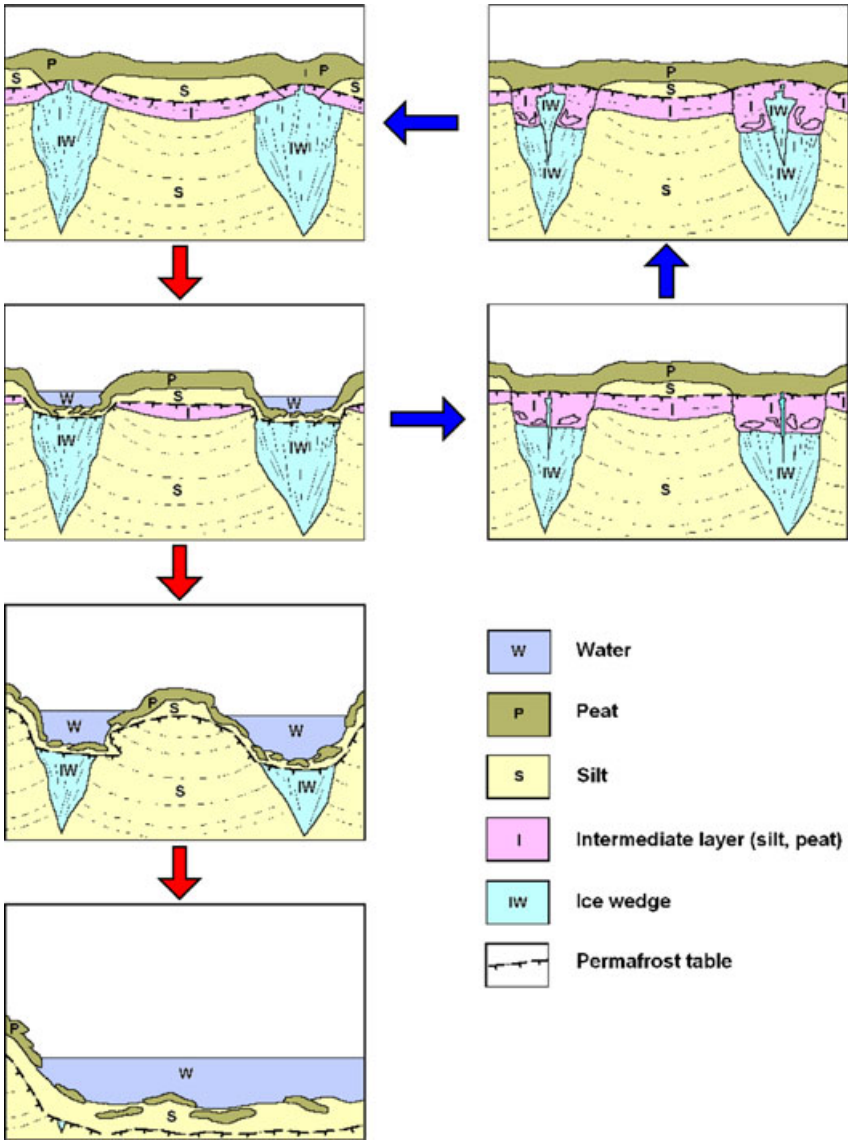

Fig. 9 Two possible thermokarst scenarios associated with ice-wedge polygon terrains. A stable or reversible process (blue arrows) is often observed in natural environments. The centers of the polygons remain stable because the protective insulative mat of vegetation and organic soils remains undisturbed. An unstable or irreversible pathway (red arrows) leads to larger water bodies and lakes if the central parts of the polygons experience thaw settlement. This can occur when the thermal insulating properties of the vegetation and organic soils are reduced due to disturbance, accumulation of road dust, or infrastructure-related flooding, resulting in increases in the thickness of the active layer.

release of nutrients and wetter soils. The mineral and organic matter insulates the trough bottoms and slows the thawing of ice wedges, eventually stabilizing the landscape in a new configuration with higher centers and deeper troughs. In areas with cold climates, a new generation of ice wedges may start to form. These wedges penetrate into the previous generation of wedges that were truncated by thermokarst (Fig. 9, two right boxes with blue arrows). If the climate remains favorable for ice wedge growth, the melted wedge-ice eventually reforms and returns the landscape to its original condition.

The second (unstable or irreversible) scenario (Fig. 9, red arrows) usually occurs where there is disturbance to the central part of the polygons, as often occurs in areas in close proximity to infrastructure. This scenario is more severe because the reduction in the protective organic layer can lead to thawing of the upper permafrost in the polygon center, rapid erosion of the edges of the polygon, and subsidence of the entire polygon. Further thermokarst development results in continuing ground subsidence, and to the formation of a shallow thermokarst pond above the polygons. This leads to accelerated thermokarst and relatively fast degradation of ice-rich soils under the pond.

Consequences to ecological systems

The areas that have been affected by extensive thermokarst in the PBO exhibit major ecological changes. No detailed plot-based studies of vegetation changes related to the transformed landscapes were available for this report, but a photographic survey of the roadside areas in map B in summer 2013 showed that numerous areas that were previously low-centered polygons as late as 1983 have been converted to well-drained high-centered polygons. The redistribution of water on the tundra surface has changed the plant communities. The vegetation in the centers of the polygons has been converted from a wet sedge, moss tundra to either a moist sedge, prostrate dwarf-shrub, moss tundra or, in more extreme situations particularly near heavily traveled roads where there has been continuous input of dust for the past 40 years, to a dry prostrate dwarf-shrub, grass, forb tundra (Fig. 2) (Walker, 1985). Many low-centered polygon troughs that previously had wet sedge, moss tundra are now ponds with up to a meter of water with either no vegetation or with aquatic sedges.

The thermokarst terrain is more topographically complex than the initial condition. The changes in hydrology and vegetation undoubtedly affect the distribution and abundance of a wide variety of organisms including insects, shorebirds, waterfowl, small mammals such as voles and lemmings , and could in turn affect the patterns of use by prey species (Batzli & Jung, 1980; Brown *et al*., 2007). Increases in surface water may increase the habitat of some waterfowl species harvested by village residents of the region (Ward *et al*., 2005). The implications of thermokarst on the habitat and distribution of fish species, such as the three-spined stickleback (*Gasterosteus aculeatus*) and broad whitefish (*Coregonus nasus*), are not well-understood, nor are the overall effects on lakes and outputs to streams and rivers. Surface water distribution and extent, and connectivity among water bodies influence fish abundance by affecting their access to seasonally important overwintering, spawning, and rearing habitats (M. Wipfli, personal communications). The altered hydrology associated with widespread thermokarst formation also has implications for tundra CO_2 and methane exchanges (Schuur *et al*., 2009; Sturtevant *et al*., 2012).

Consequences to engineered and social systems

The negative consequences of thermokarst to infrastructure are well-known and extensively documented (US Arctic Research Commission Permafrost Task Force, 2003; Streletskiy *et al*., 2012). The additional maintenance and replacement costs due to climate change on public infrastructure in Alaska is estimated at $3.6–6.1 billion through 2030, but it is difficult to isolate the projected costs of thermokarst from other climate change effects (Larsen *et al*., 2008). Within the PBO, thermokarst affects rehabilitation efforts at sites where gravel has been removed (e.g. former gravel pad or road) and trenches where cables and pipelines are buried, resulting in subsidence that greatly exacerbates the cost of rehabilitation (Streever, 2012).

Situations similar to those in the PBO also occur in villages. High-resolution satellite images show that thermokarst has become extensive within the village road network at Nuiqsut, west of the PBO. Deeper thermokarst (up to 2 m) occurs in the sandy eolian deposits west of the Colville River (Lawson *et al*., 1978), and much deeper thermokarst (up to 5.5 m) occurs in the thick, silty, organic-rich, and extremely ice-rich *yedoma* deposits of the northern Arctic Foothills (Lawson, 1983; Carter, 1988; Kanevskiy *et al*., 2011; Shur *et al*., 2012). Apart from current rough projections of costs related to relocation of Alaskan villages facing erosion problems, we are unaware of any cost estimates for private or industrial infrastructure on the North Slope related to thawing permafrost. Future effects are difficult to predict especially when combined with simultaneous rapid changes to climate, political, and socio-economic factors, and oil drilling technology.

Value of long-term studies of a rapidly changing ecosystem

When the PBO studies began in the 1970s, none of the now-senior authors who were involved foresaw the possibility of the rapid transitions that are occurring now. For over 20 years, the areas that were not affected by oilfield infrastructure showed little change. Based on the mapped information and current air and permafrost temperature trends, starting in 1990 we are witnessing landscape changes that will have major implications for much of the Arctic Coastal Plain. The conceptual model of thermokarst formation presented here and the description of the characteristics of areas most vulnerable to thermokarst will help in the development of predictive models of how thermokarst spreads in different climate-change and infrastructure scenarios.

Acknowledgments

Bill Streever provided valuable contributions to the industry portions of the paper. The late Honorable F. Geoffrey Larminie OBE (1929-2008), manager of Alaska Operations for the BP Oil Corporation in the 1970s, supported our early efforts. This work would not have been possible without the support of the BP Alaska Prudhoe Bay Unit and Aerometric Inc., which provided the GIS, aerial-photo data, and analysis of the regional infrastructure. We thank Roger Ruess and Terry Chapin for their valuable reviews. The work was funded by grants and contracts provided by the State of Alaska, National Science Foundation, US Army Cold Regions Research and Engineering Laboratory, US Fish and Wildlife Service, National Aeronautics and Space Administration, and the oil industry. Funds for the latest map analysis and preparation of this manuscript were provided by the Maps and Locals (MALS) project [NSF Grant No. 1026843, to the Arctic Long Term Ecological Research (LTER) project], the ArcSEES program, Alaska EPSCoR NSF award #OIA-1208927, and the NASA Land-Cover Land-Use Change program (Award No. NNX09AK56G).

References

ACIA (2005) *Impacts of a Warming Arctic: Arctic Climate Impact Assessment*. Cambridge University Press, Cambridge, UK.

Alaska Oil and Gas Association (2012) AOGA – Facts and Figures. Available at: http://aog@org. (accessed 10 July 2013).

AMAP (2010) *Assessment 2007: Oil and Gas Activities in the Arctic – Effects and Potential Effects*, Vol 1 and 2. Arctic Monitoring and Assessment Programme, Oslo, Norway.

Ambrosius K (2003) Appendix E: Aeromap analyses and data. In: *Cumulative Environmental Effects of Oil and Gas Activities on Alaska's North Slope* (ed. National Research Council), pp. 190–207. National Academies Press, Washington, DC, USA.

Batzli GO, Jung H-JG (1980) Nutritional ecology of microtine rodents: resource utilization near Atkasook, Alaska. *Arctic and Alpine Research*, **12**, 483–499.

Benson C, Holmgren B, Timmer R, Weller G, Parrish S (1975) Observations on the seasonal snow cover and radiation climate at Prudhoe Bay, Alaska during 1972. In: *Ecological Investigations of the Tundra Biome at Prudhoe Bay, Alaska* (ed. Brown J), pp. 12–50. Biological Papers of the University of Alaska, Special Report 2, Fairbanks, AK, USA.

Bhatt US, Walker DA, Raynolds MK *et al.* (2010) Circumpolar Arctic tundra vegetation change is linked to sea ice decline. *Earth Interactions*, Paper 14–008.

Brown J (ed.) (1975) *Ecological investigations of the tundra biome in the Prudhoe Bay region, Alaska*. Special Report No. 2, Biological Papers of the University of Alaska, Fairbanks, AK, USA.

Brown J (1980) *An Arctic Ecosystem*. Dowden, Hutchinson & Ross, New York, NY, USA.

Brown J, Hinkel KM, Nelson FE (2000) The circumpolar active layer monitoring (CALM) program: research designs and initial results. *Polar Geography*, **24**, 165–258.

Brown S, Bart J, Lanctot RB, Johnson JA, Kendall S, Payer D, Johnson J (2007) Shorebird abundance and distribution on the coastal plain of the Arctic National Wildlife Refuge. *The Condor*, **109**, 1–14.

Callaghan TV, Bjorn LO, Chapin FS III *et al.* (2005) Arctic tundra and polar desert ecosystems. In: *Arctic Climate Impact Assessment – Scientific Report* (eds Symon C, Arris L, Heal B), pp. 243–352. Cambridge University Press, Cambridge, UK.

Carter LD (1988) Loess and deep thermokarst basins in arctic Alaska. In: *Proceedings of the Fifth International Conference on Permafrost*, pp. 706–711. Tapir Publishers, Trondheim, Norway.

Epstein HE, Raynolds MK, Walker DA, Bhatt US, Tucker CJ, Pinzon JE (2012) Dynamics of aboveground phytomass of the circumpolar Arctic tundra during the past three decades. *Environmental Research Letters*, **7**, 015506.

Everett KR (1980a) Landforms. In: *Geobotanical Atlas of the Prudhoe Bay Region, Alaska, CRREL Report 80-14* (eds Walker DA, Everett KR, Webber PJ, Brown J), pp. 14–19. Army Corps of Engineers, Cold Regions Research and Engineering Laboratory, Hanover, NH, USA.

Everett KR (1980b) Geology and permafrost. In: *Geobotanical Atlas of the Prudhoe Bay Region, Alaska, CRREL Report 80-14* (eds Walker DA, Everett KR, Webber PJ, Brown J), pp. 8–9. Army Corps of Engineers, Cold Regions Research and Engineering Laboratory, Hanover, NH, USA.

Everett KR, Parkinson RJ (1977) Soil and landform associations, Prudhoe Bay area, Alaska. *Arctic and Alpine Research*, **9**, 1–19.

Forbes BC, Stammler F, Kumpula T, Meschtyb N, Pajunen A, Kaarlejärvi E (2009) High resilience in the Yamal-Nenets social-ecological system, West Siberian Arctic, Russia. *Proceedings of the National Academy of Sciences*, **106**, 22041–22048.

French HM (1976) *The Periglacial Environment*. Longman, London and New York.

Gilders MA, Cronin MA (2000) Chapter 2 – North Slope oil field development. In: *The Natural History of an Arctic Oil Field* (eds Truett JC, Johnson SR), pp. 15–33. Academic Press, San Diego, CA, USA.

Gold LW, Lachenbruch AH (1973) Thermal conditions in permafrost. A review of the North American literature. In: *North American Contribution to the Second International Conference on Permafrost*, pp. 3–23. National Academy Press, Washington, DC, USA.

Grosse G, Harden J, Turetsky M *et al.* (2011) Vulnerability of high latitude soil carbon in North America to disturbance. *Journal of Geophysical Research – Biogeosciences*, **116**, G00K06.

Jia GJ, Epstein HE, Walker DA (2003) Greening of arctic Alaska, 1981–2001. *Geophysical Research Letters*, **30**, 2067.

Jorgenson MT, Shur YL, Pullman ER (2006) Abrupt increase in permafrost degradation in Arctic Alaska. *Geophysical Research Letters*, **25**, L02503.

Kanevskiy M, Shur Y, Fortier D, Jorgenson MT, Stephani E (2011) Cryostratigraphy of late Pleistocene syngenetic permafrost (yedoma) in northern Alaska, Itkillik River exposure. *Quaternary Research*, **75**, 584–596.

Kanevskiy M, Shur Y, Jorgenson MT *et al.* (2013) Ground ice in the upper permafrost of the Beaufort Sea coast of Alaska. *Cold Regions Science and Technology*, **85**, 56–70.

Kofinas G, Clark D, Hovelsrud GKL *et al.* (2013) Adaptive and transformative capacity. In: *Arctic Resilience Interim Report 2013 Arctic Council* (ed. Nilsson AE), pp. 73–95. Environment Institute and Stockholm Resilience Centre, Stockholm, Sweden.

Komárková V, McKendrick JD (1988) Patterns in vascular plant growth forms in arctic communities and environment at Atkasook, Alaska. In: *Plant Form and Vegetation Structure* (eds Werger MJA, van der Aart PJM, During HJ, Verhoeven JTA), pp. 45–70. SPB Academic Publishing, The Hague, The Netherlands.

Krupnik I, Allison I, Bell R *et al.* (2011) *Understanding Earth's Polar Challenges: International Polar Year 2007–2008*. World Climate Research Programme, World Meteorological Organization, Geneva, Switzerland.

Kumpula T, Forbes BC, Stammler F, Meschtyb N (2012) Dynamics of a coupled system: multi-resolution remote sensing in assessing social-ecological responses during 25 years of gas field development in arctic Russia. *Remote Sensing*, **4**, 1046–1068.

Larsen PH, Goldsmith S, Smith O, Wilson LM, Strzepek K, Chinowsky P, Saylor B (2008) Estimating future costs for Alaska public infrastructure at risk from climate change. *Global Environmental Change*, **18**, 442–457.

Lawson DE (1982) *Long-term modifications of perennially frozen sediment and terrain at East Oumalik, Northern Alaska*. CRREL Report 82-36, Army Cold Regions Research and Engineering Laboratory, Hanover, NH, USA.

Lawson DE (1983) Ground ice in perennially frozen sediments, northern Alaska. *Proceedings of the Fourth International Conference on Permafrost, 17–22 July 1983, University of Alaska Fairbanks*, pp. 695–700. National Academy Press, Washington, DC, USA.

Lawson DE, JJ B, Everett KR *et al.* (1978) *Tundra disturbances and recovery following the 1949 exploratory drilling, Fish Creek, Northern Alaska*. CRREL Report 78-28, Army Cold Regions Research and Engineering Laboratory, Hanover, NH, USA.

Liu L, Schaefer K, Zhang T, Wahr J (2012) Estimating 1992–2000 average active layer thickness on the Alaskan North Slope from remotely sensed surface subsidence. *Journal of Geophysical Research*, **117**, F01005.

McKendrick JD (1987) Plant succession on disturbed sites, North Slope, Alaska, U.S.A. *Arctic and Alpine Research*, **19**, 554–565.

McKendrick JD (1991) Colonizing tundra plants to vegetate abandoned gravel pads in arctic Alaska. *Advances in Ecology*, **1**, 209–223.

Myers-Smith IH, Forbes BC, Wilmking M *et al.* (2011) Shrub expansion in tundra ecosystems: dynamics, impacts, and research priorities. *Environmental Research Letters*, **6**, 045509.

Nelson FE, Anisimov OA, Shiklomanov NI (2002) Climate change and hazard zonation in the circum-Arctic permafrost regions. *Natural Hazards*, **26**, 203–225.

Orians GH, Albert T, Brown G *et al.* (2003) *Cumulative Environmental Effects of Oil and Gas Activities on Alaska's North Slope*. National Academies Press, Washington, DC.

Rawlinson SE (1993) *Surficial geology and morphology of the Alaskan central Arctic coastal plain*. Report of Investigations 93-1, Division of Geology and Geophysical Surveys, Fairbanks, AK, USA

Schuur EAG, Vogel JG, Crummer KG, Lee H, Strickman O, Osterkamp TE (2009) The effect of permafrost thaw on old carbon release and net carbon exchange from tundra. *Nature*, **459**, 556–559.

Sellmann PV, Brown J, Lewellen RI, McKim H, Merry C (1975) *The classification and geomorphic implications of thaw lakes on the Arctic Coastal Plain, Alaska*. CRREL Research Report 334, Army Cold Regions Research and Engineering Laboratory, Hanover, NH, USA.

Shiklomanov NI, Streletskiy DA, Nelson FE (2012) Northern Hemisphere Component of the Global Circumpolar Active Layer Monitoring (CALM) Program. In: *Proceedings of the Tenth International Conference on Permafrost, Salekhard, Russia, 25–29 Jun 2012*, Vol 1 (ed. Hinkle KM), pp. 377–382. The Northern Publisher, Salekhard, Russia.

Shur Y (1988) *Upper Permafrost and Thermokarst*. Nauka, Novosibirsk. (In Russian)

Shur YL, Jorgenson MT (2007) Patterns of permafrost formation and degradation in relation to climate and ecosystems. *Permafrost and Periglacial Processes*, **18**, 7–19.

Shur Y, Osterkamp TE (2007) *Thermokarst*. Report No. INE0611, Institute of Northern Engineering, University of Alaska Fairbanks, Fairbanks, AK, USA

Shur Y, Kanevskiy M, Jorgenson T, Dillon M, Stephani E, Bray M, Fortier D (2012) Permafrost degradation and thaw settlement under lakes in yedoma environment. In: *Proceedings of the Tenth International Conference on Permafrost, 25–29 Jun 2012*, Vol 1 (ed. Hinkle KM), pp. 383–388. The Northern Publisher, Salekhard, Russia.

Streever B (2012) Ice-rich permafrost and the rehabilitation of tundra on Alaska's North Slope: lessons learned from case studies. In: *Proceedings of the Tenth International Conference on Permafrost, Salekhard, Russia, 25–29 Jun 2012*, Vol 4 (ed. Hinkle KM), pp. 573–574. The Northern Publisher, Salekhard, Russia.

Streever B, Suydam R, Payne JF *et al.* (2011) Environmental change and potential impacts: applied research priorities for Alaska's North Slope. *Arctic*, **64**, 390–397.

Streletskiy D, Shiklomanov N, Hatleberg E (2012) Infrastructure and a changing climate in the Russian Arctic: a geographic impact assessment. In: *Proceedings of the Tenth International Conference on Permafrost, Salekhard, Russia, 25–29 Jun 2012*, Vol 1 (ed. Hinkle KM), pp. 407–412. The Northern Publisher, Salekhard, Russia.

Sturm M, Racine C, Tape K (2001) Increasing shrub abundance in the Arctic. *Nature*, **411**, 3.

Sturtevant CS, Oechel WC, Zona D, Kim Y, Emerson CE (2012) Soil moisture control over autumn season methane flux, Arctic Coastal Plain of Alaska. *Biogeosciences*, **9**, 1423–1440.

Tape KD, Hallinger M, Welker JM, Ruess RW (2012) Landscape heterogeneity of shrub expansion in Arctic Alaska. *Ecosystems*, **15**, 711–724.

Truett JC, Johnson SR (2000) *The Natural History of an Arctic Oil Field*. Academic Press, San Diego, CA, USA.

U.S. Arctic Research Commission Permafrost Task Force (2003) *Climate change, permafrost, and impacts on civil infrastructure*. Special Report 01-03, Arctic Research Commission, Arlington, VA, USA.

USEIA (2012) *Annual Energy Outlook*, pp. 1–252. US Department of Energy, Washington, DC.

Van Everdingen RO (ed.) (1998) *Multi-Language Glossary of Permafrost Related Groundice Terms*. University of Alberta, Calgary, AB, Canada.

Walker DA (1985) *Vegetation and environmental gradients of the Prudhoe Bay region, Alaska*. CRREL Report 85-14, Army Cold Regions Research and Engineering Laboratory, Hanover, NH, USA.

Walker DA (1996) Disturbance and recovery of Arctic Alaskan vegetation. In: *Landscape Function and Disturbance in Arctic Tundra* (eds Reynolds JF, Tenhunen JD), pp. 35–71. Springer-Verlag, Heidelberg, Berlin.

Walker DA (1997) Arctic Alaskan vegetation disturbance and recovery: a hierarchic approach to the issue of cumulative impacts. In: *Disturbance and Recovery in Arctic Lands* (ed. Crawford RMM), pp. 457–479. Kluwer Academic Publishers, Dordrecht, The Netherlands.

Walker DA (2000) Hierarchical subdivision of arctic tundra based on vegetation response to climate, parent material, and topography. *Global Change Biology*, **6**, 19–34.

Walker DA, Everett KR (1987) Road dust and its environmental impact on Alaskan taiga and tundra. *Arctic and Alpine Research*, **19**, 479–489.

Walker DA, Everett KR (1991) Loess ecosystems of northern Alaska: regional gradient and toposequence at Prudhoe Bay. *Ecological Monographs*, **61**, 437–464.

Walker DA, Everett KR, Webber PJ, Brown J (eds.) (1980) *Geobotanical atlas of the Prudhoe Bay region, Alaska*. CRREL Report 80-14, Army Corps of Engineers, Cold Regions Research and Engineering Laboratory, Hanover, NH, USA

Walker DA, Binnian EF, Lederer ND, Nordstrand EA, Meehan RH, Walker MD, Webber PJ (1986a) *Cumulative landscape impacts in the Prudhoe Bay Oil Field 1949–1983*. Final Report Interagency Agreement No. DE-A106-84RL10584, Fish and Wildlife Service, Anchorage, AK, USA.

Walker DA, Webber PJ, Walker MD, Lederer ND, Meehan RH, Nordstrand EA (1986b) Use of geobotanical maps and automated mapping techniques to examine cumulative impacts in the Prudhoe Bay Oilfield, Alaska. *Environmental Conservation*, **13**, 149–160.

Walker DA, Webber PJ, Binnian EF, Everett KR, Lederer ND, Nordstrand EA, Walker MD (1987) Cumulative impacts of oil fields on northern Alaskan landscapes. *Science*, **238**, 757–761.

Walker DA, Forbes BC, Leibman MO *et al.* (2011) Cumulative effects of rapid landcover and land-use changes on the Yamal Peninsula, Russia. In: *Eurasian Arctic Land Cover and Land Use in a Changing Climate* (eds Gutman G, Reissel A), pp. 206–236. Springer, New York, NY.

Ward DH, Reed A, Sedinger JS, Black JM, Derksen DV, Castelli PM (2005) North American Brant: effects of changes in habitat and climate on population dynamics. *Global Change Biology*, **11**, 869–880.

WRCC (2012) Western Regional Climate Center, Daily Climate Data. Available at: http://www.wrcc.dri.edu/ (accessed 26 July 2013).

Supporting Information

Additional Supporting Information may be found in the online version of this article:

Appendix S1. Ice-rich permafrost at Prudhoe Bay. By Y. Shur, M. Kanevskiy, V.E. Romanovsky, K.R. Everett, J. Brown, and D.A. Walker.

Appendix S2. Calculation of impacts of oilfield development, North Slope Alaska, by K.J. Ambrosius.

Appendix S3. Integrated Geoecological and Historical Change Mapping: history, methods, maps, and summary information, by D.A. Walker, M.K. Raynolds, P.J. Webber and J. Brown.